




Metabolomics analyses reveal the crucial role of ERK in regulating metabolic pathways associated with the proliferation of human cutaneous T-cell lymphoma cells treated with Glabridin

Abdul Q. Khan¹  | Maha Victor Agha¹ | Fareed Ahmad^{2,3} | Rasheeda Anver¹ | Khalid Sultan A. M. Sheikhan¹ | Jericha Mateo¹ | Majid Alam^{1,2,3} | Joerg Buddenkotte^{2,3} | Shahab Uddin^{1,2,4}  | Martin Steinhoff^{1,2,3,5,6,7} 

¹Translational Research Institute, Academic Health System, Hamad Medical Corporation, Doha, Qatar

²Dermatology Institute, Academic Health System, Hamad Medical Corporation, Doha, Qatar

³Department of Dermatology and Venereology, Rumailah Hospital, Hamad Medical Corporation, Doha, Qatar

⁴Laboratory Animal Research Center, Qatar University, Doha, Qatar

⁵Department of Medicine, Weill Cornell Medicine Qatar, Qatar Foundation-Education City, Doha, Qatar

⁶Department of Medicine, Weill Cornell Medicine, New York, New York, USA

⁷College of Medicine, Qatar University, Doha, Qatar

Correspondence

Abdul Q. Khan and Martin Steinhoff, Translational Research Institute, Academic Health System Hamad Medical Corporation, P.O. Box 3050, Doha, Qatar.

Email: akhan42@hamad.qa and msteinhoff@hamad.qa

Funding information

Hamad Medical Corporation, Grant/Award Number: MRC-01-23-067

Abstract

Cutaneous T-cell lymphomas (CTC) are a heterogeneous group of T-cell lymphoproliferative malignancies of the skin with limited treatment options, increased resistance and remission. Metabolic reprogramming is vital in orchestrating the uncontrolled growth and proliferation of cancer cells. Importantly, deregulated signalling plays a significant role in metabolic reprogramming. Considering the crucial role of metabolic reprogramming in cancer-cell growth and proliferation, target identification and the development of novel and multi-targeting agents are imperative. The present study explores the underlying mechanisms and metabolic signalling pathways associated with Glabridin mediated anti-cancer actions in CTCL. Our results show that Glabridin significantly inhibits the growth of CTCL cells through induction of programmed cell death (PCD) such as apoptosis, autophagy and necrosis. Interestingly, results further show that Glabridin induces PCD in CTCL cells by targeting MAPK signalling pathways, particularly the activation of ERK. Further, Glabridin also sensitized CTCL cells to the anti-cancer drug, bortezomib. Importantly, LC-MS-based metabolomics analyses further showed that Glabridin targeted multiple metabolites and metabolic pathways intricately involved in cancer cell growth and proliferation in an ERK-dependent fashion. Overall, our findings revealed that Glabridin induces PCD and attenuates the expression of regulatory proteins and metabolites involved in orchestrating the uncontrolled proliferation of CTCL cells through ERK activation. Therefore, Glabridin possesses important features of an ideal anti-cancer agent.

1 | INTRODUCTION

Cancer is a complex and heterogeneous disease with exponentially increasing incidence, deaths and morbidity, posing a huge

socio-economic burden to patients and their relatives. In this line, skin cancer is a major health problem and is increasing at an alarming rate. Basal cell carcinoma and squamous cell carcinoma are the two major types of skin cancer. Cutaneous T-cell lymphomas (CTCL), a

This is an open access article under the terms of the [Creative Commons Attribution](https://creativecommons.org/licenses/by/4.0/) License, which permits use, distribution and reproduction in any medium, provided the original work is properly cited.

© 2024 The Author(s). *Cell Proliferation* published by Beijing Institute for Stem Cell and Regenerative Medicine and John Wiley & Sons Ltd.

2.3 | Cell culture

Human cutaneous T-cell lymphoma cell lines, HH and H9 were acquired from the American Type Culture Collection (ATCC), 10801 University Boulevard Manassas, VA 20110, USA. Cells were cultured in Roswell Park Memorial Institute (RPMI) 1640 Medium supplemented with 10% (v/v) fetal bovine serum (FBS), 100 U/mL penicillin and 100 U/mL streptomycin at 37°C in a humidified atmosphere containing 5% CO₂. Treatments were done in a 5% RPMI medium.

2.4 | Cell counting kit-8 (CCK-8) assay

The anti-proliferative/cytotoxic action of Glabridin, bortezomib and or pharmacological inhibitors in CTCL cells was done using the Cell Counting Kit-8 (CCK-8) assay as described earlier.³⁰

2.5 | Annexin V staining

CTCL cells were treated with Glabridin alone and or in combination with bortezomib or the ERK inhibitor. After 24 h of the treatment, cells were harvested and washed with phosphate-buffered saline (PBS). To measure the frequency of apoptotic cells, roughly 500,000 cells were stained with fluorescein-conjugated annexin V antibody and propidium iodide for 30 min at room temperature in an annexin binding buffer. Around 300,000 stained cells were acquired by flow cytometry (BD LSRFortessa analyser, BD Biosciences). To find out the frequencies of apoptotic and necrotic cells, FCS3 files of the recorded data were analysed using FlowJo (version10.7.1) software.

2.6 | Measurement of mitochondrial membrane potential

HH and H9 cells were treated with Glabridin alone and or in combination. After 24 h of the treatment, cells were harvested, washed and finally stained (500,000 cells) with a JC1 stain kit for 30 min at room temperature as per the manufacturer's instruction (ThermoFisher) and then analysed using flow cytometry (BD LSR Fortessa analyser, BD Biosciences, USA).

2.7 | Cell cycle analysis

HH and H9 cells were treated with Glabridin for 24 h. Thereafter, cells were harvested and fixed using 100% ethanol overnight at 4°C. The next day, cells were washed using HBSS and resuspended in 250 µL of PI/RNase solution (BD Biosciences) for 15 min at room temperature. After incubation, cells were washed and resuspended in 300 µL of HBSS. Cells were acquired on a flow cytometer BD LSRFortessa cell analyser and analysed as mentioned above.

2.8 | Live/dead assay

CTCL cells were treated with Glabridin alone and or in combination with ERK inhibitor for 24 h and then stained with LIVE/DEAD, viability/cytotoxicity Kit from Thermo Fisher Scientific as described previously.³⁰ Briefly, Live/dead stains were prepared, and cells were stained according to the kit protocol. Finally, cells were visualized, and images were captured using the EVOS FLc cell imaging system.

2.9 | Cell lysis and immunoblotting

To investigate the underlying molecular mechanism of Glabridin-mediated anti-cancer actions in CTCL, cells were treated with Glabridin alone and or in combination with bortezomib/ERK inhibitor/ZVAD-FMK, 3MA and so forth and immunoblotting was performed as described previously.³⁰ Briefly, treated, and untreated cells were harvested and washed with PBS followed by cell lysis and determination of the protein concentration. Proteins were separated using SDS-PAGE and transferred to polyvinylidene difluoride (PVDF) membrane followed by blocking and incubation with primary antibodies at 4°C overnight. Next morning, blots were washed and incubated with secondary antibodies and finally after washing blots were visualized under a Chemi-Doc System (Bio-Rad, Hercules, California, USA) using ECL.

2.10 | Spheroid culture

Spheroids were generated in the lab in the form of spheres. Initially, cells were grown in normal 10% RPMI media. Then for the sphere generation, cells were cultured and treated in ultra-low attachment plates/flasks (Corning, USA) using the complete cancer stem cell medium (3D Tumorsphere Medium XF, Promo Cell, Germany, C-28070) at 37°C in a humidified chamber containing 5% CO₂. Cells were monitored regularly and after 7 days, spheres were photographed using EVOS FL imaging system from Invitrogen (Thermo Fisher Scientific) 4× magnification.

2.11 | Targeted metabolomics and data analysis

Metabolomic profiling of the CTCL cells treated with Glabridin was performed using the MxP[®] Quant 500 kit (Biocrates Life Sciences AG, Innsbruck, Austria) with an UHPLC-MS/MS system, which consists of an ultra-High-Performance Liquid Chromatography (UHPLC) and a Triple Quad 5500+ MS/MS system (SCIEX, Framingham, MA, USA). Data were acquired from flow injection analysis (FIA), and liquid chromatography (LC) methods in both positive and negative ionization modes to accomplish the identification and quantification of metabolites according to the manufacturer's instructions as described previously.³¹ In brief, 10 µL samples (Cell Lysate),

calibration standards, quality control samples (provided with the kit) and zero samples were transferred to each predefined well of the 96-well filter plate that contains internal standards. Next, the kit plate was dried and incubated with 5% phenyl-isothiocyanate to derivatize amino acids and biogenic amines in all the samples. Then, the plate with derivatized samples was dried using the Ultravap Mistral (Porvair Sciences) and analytes were eluted with 5 mmol/L ammonium acetate in methanol followed by dilution (two-fold for LC-MS/MS and 50-fold for FIA-MS/MS) and finally the samples were analyzed by UHPLC-MS/MS system. We used MxP[®] Quant 500 kit LC column system (Biocrates) with the gradient mobile phases A: 0.2% formic acid in water and B: 0.2% formic acid in acetonitrile. All the parameters including the run time, ionization, voltages, temperatures, and the detection of m/z pair precursor and product ion at multiple reaction monitoring (MRM) mode were set as per the MxP[®] Quant 500 kit method. Data were recorded using the Analyst software (SCIEX) and transferred to the MetIDQ software (Biocrates) for further data processing. Further analysis, including data normalization, univariate and multivariate statistics, metabolite enrichment and pathway analysis was done using MetaboAnalyst 6.0 (<https://www.metaboanalyst.ca/>).³²

2.12 | Statistical analysis

Data from various experimental groups are presented as mean \pm SD. Statistical calculations (ANOVA, post hoc test) were performed by using GraphPad Prism (GraphPad Software Inc., San Diego, CA, <http://www.graphpad.com>). Values of $*p < 0.05$ were considered statistically significant.

3 | RESULTS

3.1 | Glabridin inhibits CTCL cell viability

Deregulated programmed cell death (PCD) is a key factor in orchestrating the acquisition of cancer hallmarks, and hence requires further investigation. In this line, we first treated the human CTCL cells with Glabridin at different concentrations (0, 2.5, 5, 10, 20, 40 and 80 μ M) for 24 h, followed by CCK-8 based cell viability test and interestingly our results showed a significant reduction in the percentage cell viability in CTCL cells (HH and H9) ($p < 0.0001$) (Figure 1A,B). Further, we also compared the cytotoxic effect of Glabridin with well-known anti-cancer drugs, doxorubicin and azacytidine (Supplementary Figure S1A,B). Next, we also observed a notable change in the intracellular (nucleus) as well as in the cell membrane as demonstrated by the live and dead cell staining in Glabridin treated HH (Figure 1C) and H9 (Figure 1D) cells. In line, Glabridin treatment significantly altered the cell cycle distribution pattern, which resulted in the accumulation of cells/cell arrest at the sub G0-G1 phase in HH and H9 cells (Supplementary Figure S1C-F). Moreover, Glabridin also causes a

significant decrease in mitochondrial membrane potential (MMP) in CTCL cells (Supplementary Figure S2A-D). Indeed, flow cytometry data of FITC Annexin V and PI staining, to identify cell death and determine apoptosis and necrosis, also showed that Glabridin treatment results in a significantly increased number of apoptotic and necrotic cells (Figure 1E-H) and hence supports its anti-proliferative potential. Considering the growth inhibitory effects of Glabridin, we explored the associated underlying mechanism and our data showed activated p-H2AX and HMGB1 (Figures 1I-L and 2A-D). HMGB1 (High Mobility Group Box 1 protein) is a ubiquitous non-histone nuclear protein, passively released by the necrotic cells. Thus, these data indicate the potential of Glabridin as an inducer of PCD in CTCL cells.

3.2 | Glabridin activates apoptosis in CTCL cells

Considering the strong anti-proliferative potential of Glabridin, we explored the status of the regulatory proteins associated with apoptosis. Interestingly, Glabridin-mediated apoptosis through upregulation/activation of cleaved caspase-3 in CTCL cells as indicated in Figure 2E-H. Indeed, the expression of poly ADP ribose polymerase (PARP), a DNA damage repair enzyme, is also significantly altered by Glabridin in CTCL cells (Figure 2I-L).

Next, we used z-VAD-FMK, a pan-caspase inhibitor to confirm the role of apoptosis in Glabridin-induced CTCL cell death. As shown in Supplementary Figure S3A-H, z-VAD-FMK reversed the Glabridin-induced apoptosis as evident from the expression of apoptotic markers and hence supports the crucial role of apoptosis in Glabridin treated CTCL cells.

3.3 | Glabridin induces autophagy in CTCL cells

Autophagy, another type of PCD, plays a crucial role in cellular and biological homeostasis, often supporting cancer cell survival and growth. Keeping this in mind, we explored the role of autophagy in Glabridin-treated CTCL cells. Indeed, our data show that Glabridin induces upregulation of autophagy, as evident from LC3 expression (Figure 3A-D). In line, our result also revealed that Glabridin causes modulation of autophagy regulatory proteins in CTCL cells (Figure 3E-H). Importantly, 3-Methyladenine (3-MA), an autophagy inhibitor, treatment reversed Glabridin mediated autophagy in CTCL cells and thus indicated the role of autophagy (Figure 3I-L). Further, we also checked the status of the apoptotic markers, caspase-3 and cleaved caspase-3 (Supplementary Figure S3I-N) and observed an increase in caspase-3 activation in CTCL cells treated with 3-MA and Glabridin. Thus, these results suggest that Glabridin induced autophagy could repress apoptosis in Glabridin treated CTCL cells, or in other words Glabridin treatment causes protective/antiapoptotic autophagy in CTCL cells and hence autophagy inhibition may enhance the apoptotic effects of Glabridin in CTCL cells.

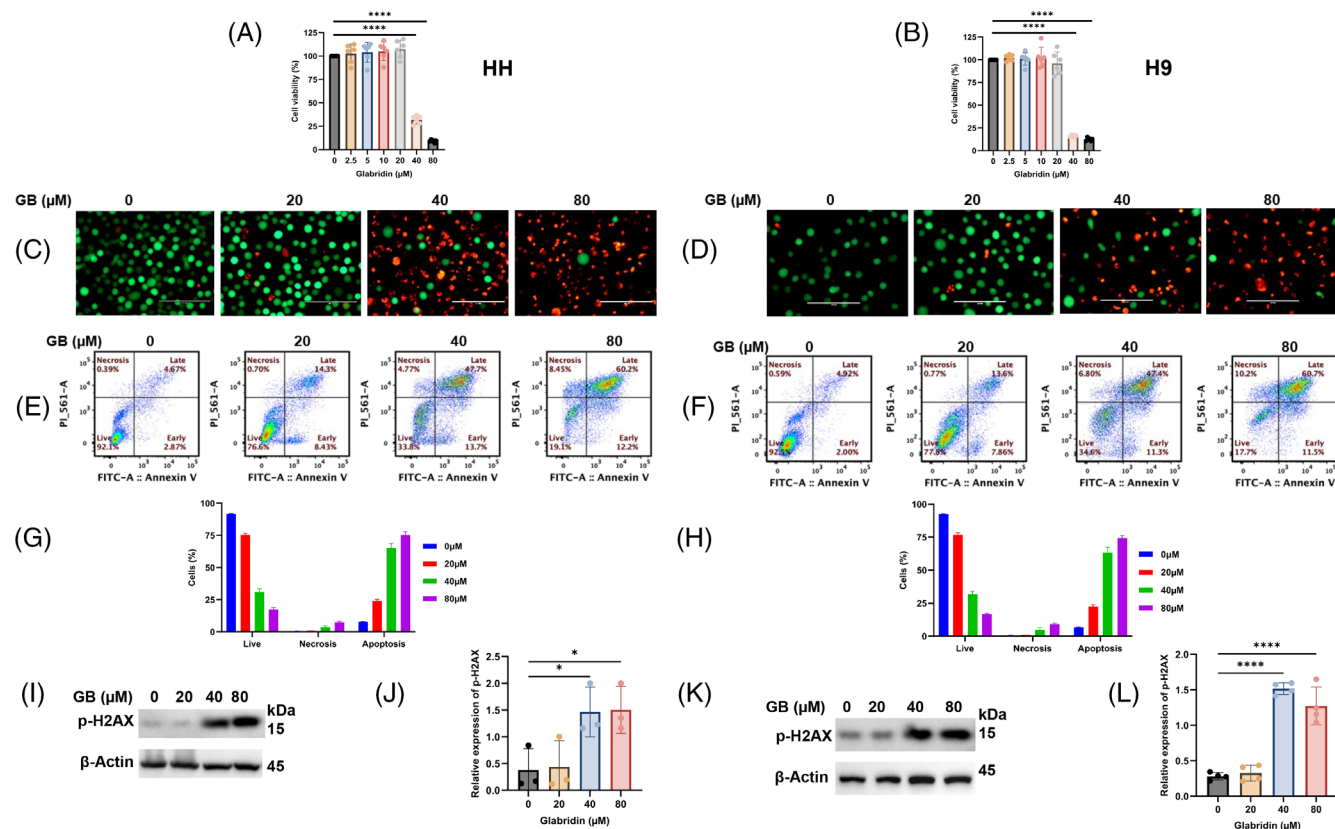


FIGURE 1 Glabridin suppressed the growth of CTCL cells. (A and B) The effect of the indicated concentration of Glabridin on the % cell viability of HH and H9 cells and data were presented as mean \pm SD ($n = 6$). (C and D) The live and dead cell staining in Glabridin treated HH and H9 cells. For the identification of live cells, we have used green, fluorescent calcein-AM dye for the intracellular esterase and red-fluorescent ethidium homodimer-1 which indicates a loss of membrane integrity (scale bar 100 μ m; magnification 40 \times). (E and F) The representative results of HH and H9 cells treated with the indicated concentrations of Glabridin for 24 h followed by staining with fluorescein-conjugated Annexin-V/PI, and apoptotic as well as necrotic cells were determined by flow cytometry ($n = 3$). (G and H) The percentage of apoptosis and necrosis in cells of the treatment groups and the data is expressed as mean \pm SD ($n = 3$). (I–L) Glabridin induced expression of DNA damage marker. HH and H9 cells were treated with Glabridin, and lysates were prepared. Detection of p-H2AX by western blot analysis and its relative quantification was presented as mean \pm SD ($n = 3$). The intensity of the bands was normalized with the respective loading control and quantified using image lab software. * $p < 0.05$ and **** $p < 0.0001$ represents the level of significance between treatment groups with respect to control.

3.4 | Glabridin modulates MAPK signalling in CTCL cells

MAPK signalling is imperative in a myriad of biological functions from the developmental stage to the growing phase and till death. Interestingly, these pathways are very much involved in the repair and prolong survival of cancer cells which often translate into cancer hallmarks such as drug resistance and limitless proliferation. Importantly, cancer therapeutic measures including phototherapy and chemotherapy also act through these pathways. Hence, we checked the role of MAPK in Glabridin-induced anti-cancer actions in CTCL cells. In this line, our results clearly show that Glabridin modulated the expression and the function of MAPK signalling. As shown in Figure 4, Glabridin markedly modulated the expression of MAPK signalling pathways (ERK, p38 and JNK). However, our results showed marked ERK activation at 40 and 80 μ M concentrations of Glabridin treatments in CTCL cells (Figure 4A–D). Moreover, we did not detect a

significant change in the expression of total ERK proteins. Interestingly, Glabridin induced activation of p-P38 and p-JNK was not consistent with its increasing concentrations (Figure 4E–L). Thus, our results suggest that Glabridin-induced modulation of MAPK pathways particularly ERK is crucial and potentially the important underlying mechanism of Glabridin.

3.5 | Glabridin induces programmed cell death in CTCL cells through ERK activation

ERK signalling is vital for the maintenance of cell growth and proliferation, and protection from endogenous as well as exogenous insults. Additionally, ERK activation is very much involved in cancer therapeutic measures, including phototherapy and chemotherapy. Hence, we wanted to explore whether Glabridin induced ERK activation is crucial in orchestrating the PCD in CTCL cells or not. To do so, we treated

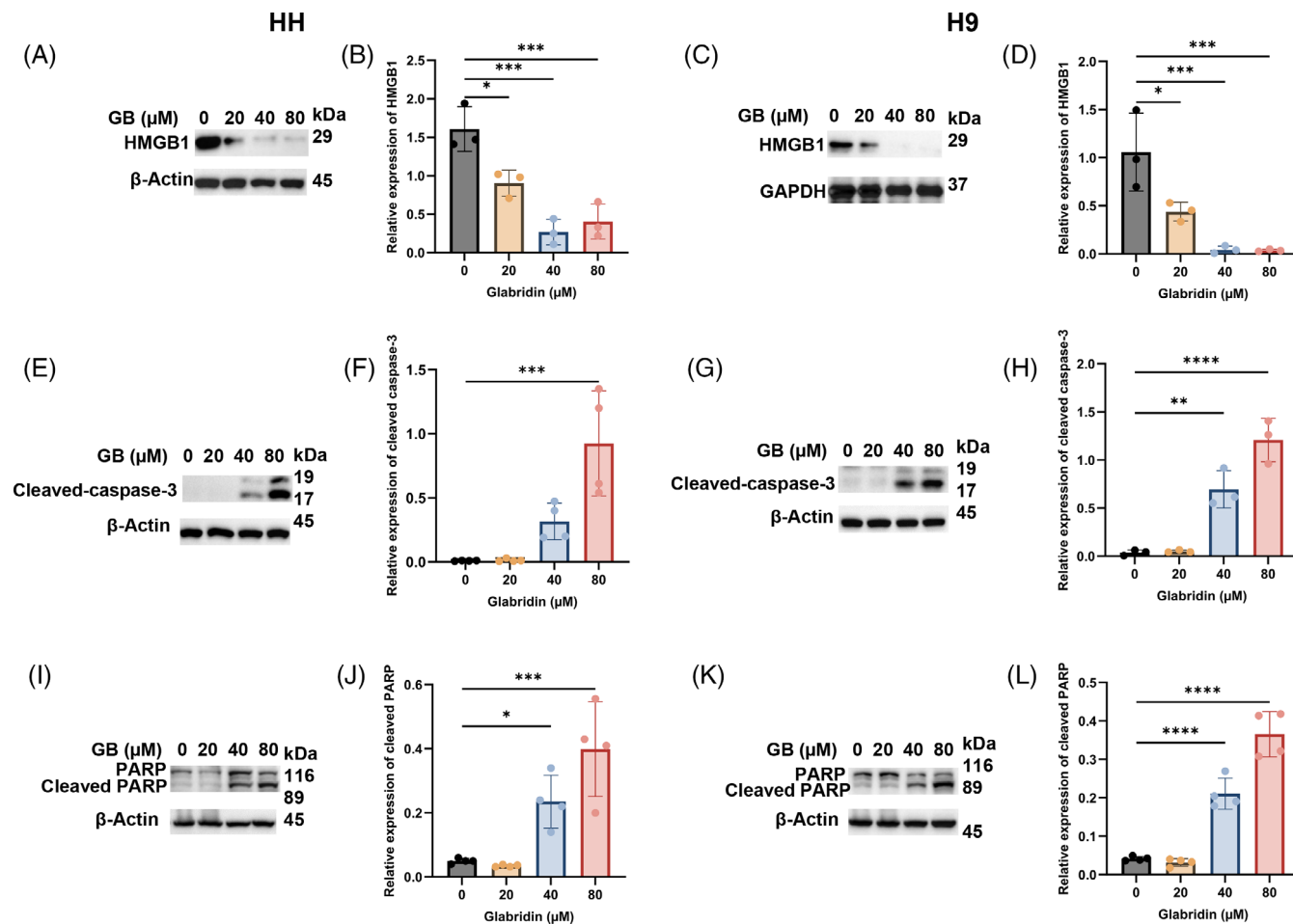


FIGURE 2 Glabridin induces cytotoxic effects through programmed cell death. CTCL cell lines, HH and H9 were treated with the indicated concentrations of Glabridin, and cell lysates were prepared and then immunoblotted. (A–L) Western blot analysis of three proteins (HMGB1, cleaved caspase-3 and PARP) and their relative quantification result are presented as mean \pm SD ($n = 3$). The intensity of the bands was normalized with the respective loading control and quantified using image lab software. * $p < 0.05$, ** $p < 0.01$, *** $p < 0.001$ and **** $p < 0.0001$ represents the level of significance between treatment groups with respect to control.

CTCL cells with PD98059, a selective inhibitor of ERK1/2 signalling, alone and in combination with Glabridin and studied various parameters. In this line, our data from live and dead cell staining showed that PD98059 markedly reversed Glabridin-induced cell death, as shown in Figure 5A,B. Next, PD98059 mediated ERK inhibition markedly reversed the number of cells in the apoptotic and necrosis stages due to Glabridin treatment in CTCL cells (Supplementary Figure S4A). This further supports the crucial role of ERK in Glabridin-mediated anticancer actions in CTCL cells. Moreover, we also checked the underlying mechanisms associated with PCD in CTCL cells treated with PD98059 alone and in combination with Glabridin. Intriguingly, the results showed a strong association of apoptosis, autophagy and necrosis with Glabridin-induced ERK activation in CTCL cells. As shown in Figure 5C–N, ERK inhibition markedly reversed the expression of proteins associated with PCD due to Glabridin treatment in CTCL cells. Thus, these results demonstrated that Glabridin induced PCD in CTCL cells is ERK-dependent.

3.6 | Metabolomics profiling of CTCL cells treated with Glabridin and ERK inhibitor PD98059

LCMS-based targeted metabolic profiling was done using the MxP Quant 500 kit (biocrates) to understand the metabolic alterations in CTCL cells treated with Glabridin and ERK inhibitor PD98059. Data normalization and statistical analysis (univariate and multivariate) were done using Metaboanalyst 6.0.³² One-way ANOVA with post hoc analysis identified 186 significantly altered features in CTCL cells treated with Glabridin and PD98059 alone and in combination (Figure 6A; Supplementary Table S1). Statistical results including f -values, p -values and FDR values of the significant features are mentioned in Supplementary Table S1. A heatmap analysis of the significant features ($p < 0.05$) also showed the differential level in various treatment groups as shown in Supplementary Figure S5A. Red represents a high concentration level of metabolite and green represents a low metabolite concentration level (Supplementary Figure S5A). We

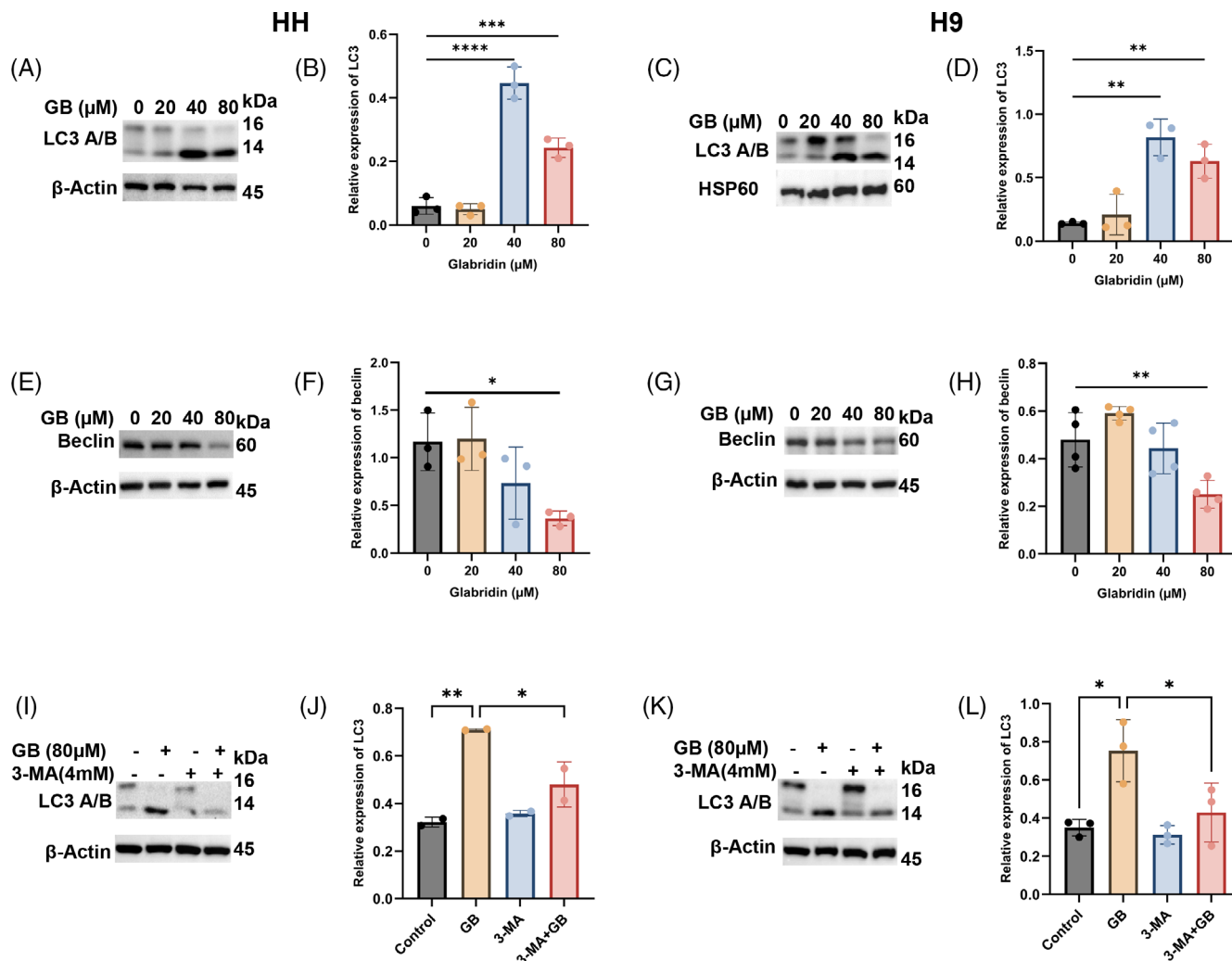


FIGURE 3 Glabridin treatment induces autophagy in CTCL cells. HH and H9 cells were treated with the indicated concentrations of Glabridin, and cell lysates were prepared and immunoblotted against autophagy markers. (A–H) Western blot analysis of LC3 and beclin and their relative quantification result are presented as mean \pm SD ($n = 3$). The intensity of the bands was normalized with the respective loading control and quantified using the image lab software. (I–L) HH and H9 cells were treated with the indicated concentration of Glabridin in the presence and absence of 3-methyladenine (3-MA) and cell lysates were prepared followed by expression analysis of LC3. Western blot analysis of LC3 and its relative quantification results are presented as mean \pm SD ($n = 3$). The intensity of the bands was normalized with the respective loading control and quantified using image lab software. * $p < 0.05$, ** $p < 0.01$, *** $p < 0.001$ and **** $p < 0.0001$ represent the level of significance between treatment groups relative to control groups.

further performed principal component analysis (PCA) which showed a clear separation of each group with a variance of the first principal component (PC1) (44%), and second principal component (PC2) (23.4%) (Figure 6B) thus demonstrating a distinct metabolic signature or a differential metabolism of cells in each treatment group. The corresponding 2D loading plot is also shown in Figure 6C. ANOVA with post hoc analysis shows the significant modulation in different categories of metabolites, including amino acid, amino acid related, biogenic amines, carboxylic acids, fatty acid, ceramides, hexosylceramides, acylcarnitines, nucleobases related and vitamins and cofactors, in Glabridin treated CTCL cells in an ERK-dependent fashion (Supplementary Figure S6A–F, Supplementary Table S1). Level of six amino acids (aspartic acid [Asp], cysteine [Cys], glycine [Gly], glutamic acid [Glu], alanine [Ala] and threonine [Thr]) and nine amino

acid related metabolites (asymmetric dimethylarginine [ADMA], 5-aminovaleric acid [5-AVA], citrulline, cystine, levodopa or dihydroxyphenylalanine [DOPA], homocysteine [Hcys], 3-methylhistidine [3-Met-His], trans-4-hydroxyproline [t4-OH-Pro] and Taurine) was significantly modulated due to Glabridin treatment and interestingly, level of all these metabolites was reversed by ERK inhibition (Supplementary Figure S6A,B and Supplementary Table S1).

Fatty acids are another important category of metabolites strongly associated with cancer pathogenesis. Metabolic profiling data revealed that arachidonic acid (AA), docosahexaenoic acid (DHA), FA(20:3) (eicosatrienoic acid) and FA(18:2) (octadecadienoic acid) level was significantly altered by Glabridin which was reversed by ERK inhibition (Supplementary Figure S6C, Supplementary Table S1). In addition, four carboxylic acids namely, aconacid (aconitic acid), Suc

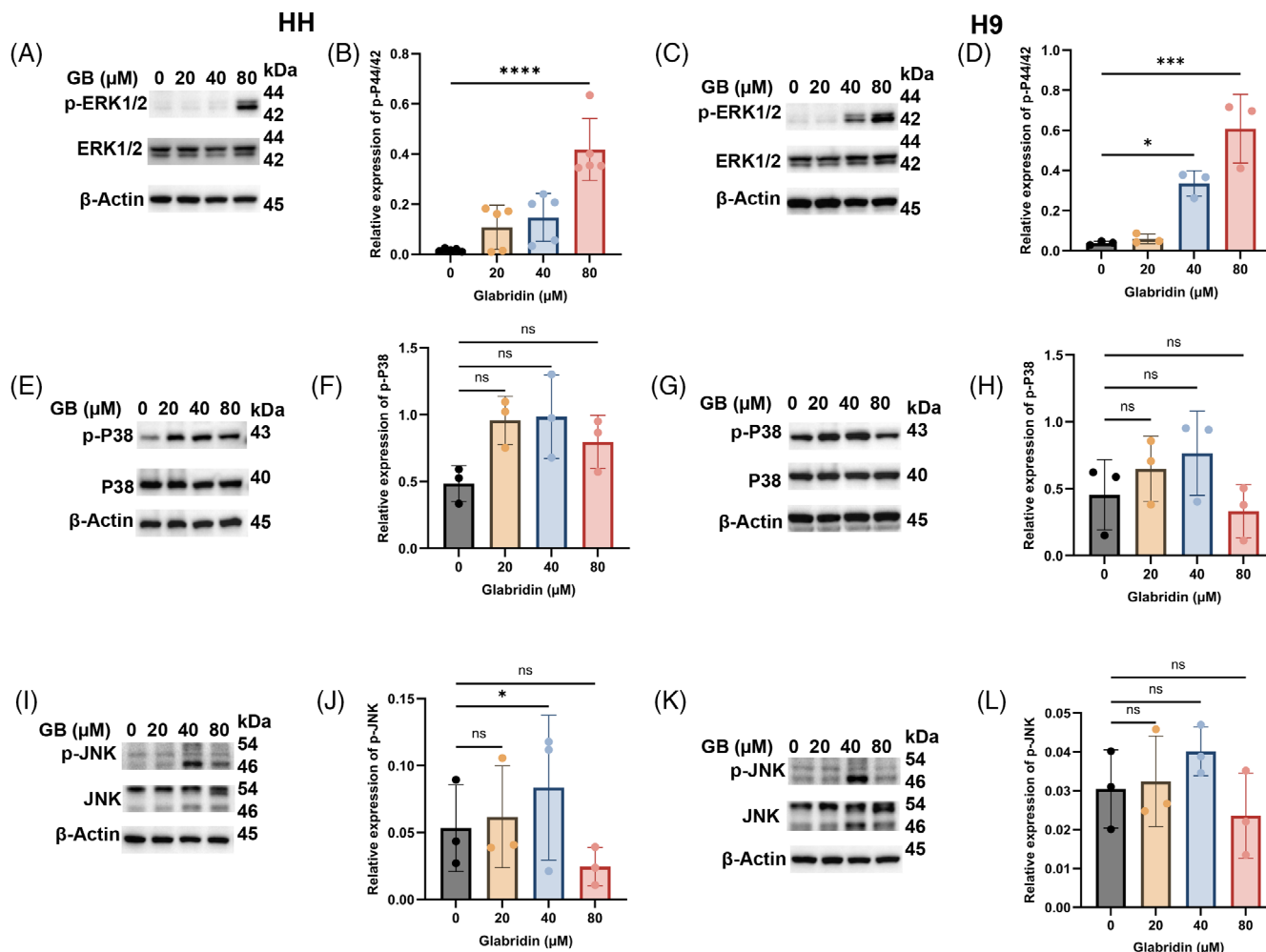


FIGURE 4 Glabridin modulates MPAK signalling pathways in CTCL. HH and H9 cells were treated with indicated concentrations of Glabridin followed by lysate preparation and immunoblotting. (A–D) Western blot analysis of p-P44/42, P44/42 and their relative quantification results are presented as mean \pm SD ($n = 3$). The intensity of the bands was normalized with the β -actin and quantified using image lab software. (E–H) Western blot analysis of p-P38, P38 and their relative quantification results are presented as mean \pm SD ($n = 3$). The intensity of the bands was normalized with the respective loading control and quantified using image lab software. (I–L) Western blot analysis of p-PJNK, JNK and their relative quantification results are presented as mean \pm SD ($n = 3$). The intensity of the bands was normalized with the respective loading control and quantified using image lab software. * $p < 0.05$, *** $p < 0.001$ and **** $p < 0.0001$ represent the level of significance between treatment groups relative to control. ns, non-significant.

(succinic acid), Lac (lactic acid) and OH-Glut acid (3-hydroxyglutaric acid) level were significantly reduced by Glabridin and was reversed due to ERK inhibition (Supplementary Figure S6D, Supplementary Table S1). Moreover, metabolites of different categories such as biogenic amines (spermine, gamma-aminobutyric acid [GABA] and β -alanine) (Supplementary Figure S6D, Supplementary Table S1), ceramides and hexocylceramides (Supplementary Figure S6E, Supplementary Table S1), acylcarnitines, choline and hypoxanthine (Supplementary Figure S6F, Supplementary Table S1), was significantly modulated by Glabridin in an ERK dependent manner. Hypoxanthine, a nucleobase purine derived metabolite, was also significantly reduced by Glabridin in CTCL cells (Supplementary Figure S6F, Supplementary Table S1).

Moreover, we also performed metabolite enrichment and pathway analysis of the significant features ($p < 0.05$), based on the Small

Molecule Pathway Database (SMPDB) database and Kyoto Encyclopedia of Genes and Genomes (KEGG) database using Metaboanalyst 6.0. respectively. Interestingly, quantitative enrichment analysis of the significant metabolites in Glabridin treated CTCL cells shows the enrichment of the significant features in several important metabolic pathways, as shown in Figure 6D. Importantly, pathway analysis reveals a total of 41 metabolic pathways modulated in Glabridin treated CTCL cells (Figure 6E; Supplementary Table S2). Importantly, thiamine metabolism, taurine and hypotaurine metabolism, glycine, serine and threonine metabolism, glutathione metabolism and cysteine and methionine metabolism are the major five metabolic pathways affected in Glabridin treated CTCL cells (Figure 6E). In line, various statistical nomenclatures, including p -value, $-\log(p)$ value, Holm- p value, false discovery rate (FDR) value and pathway impact values are mentioned in the Supplementary Table S2. Similarly, an overview of

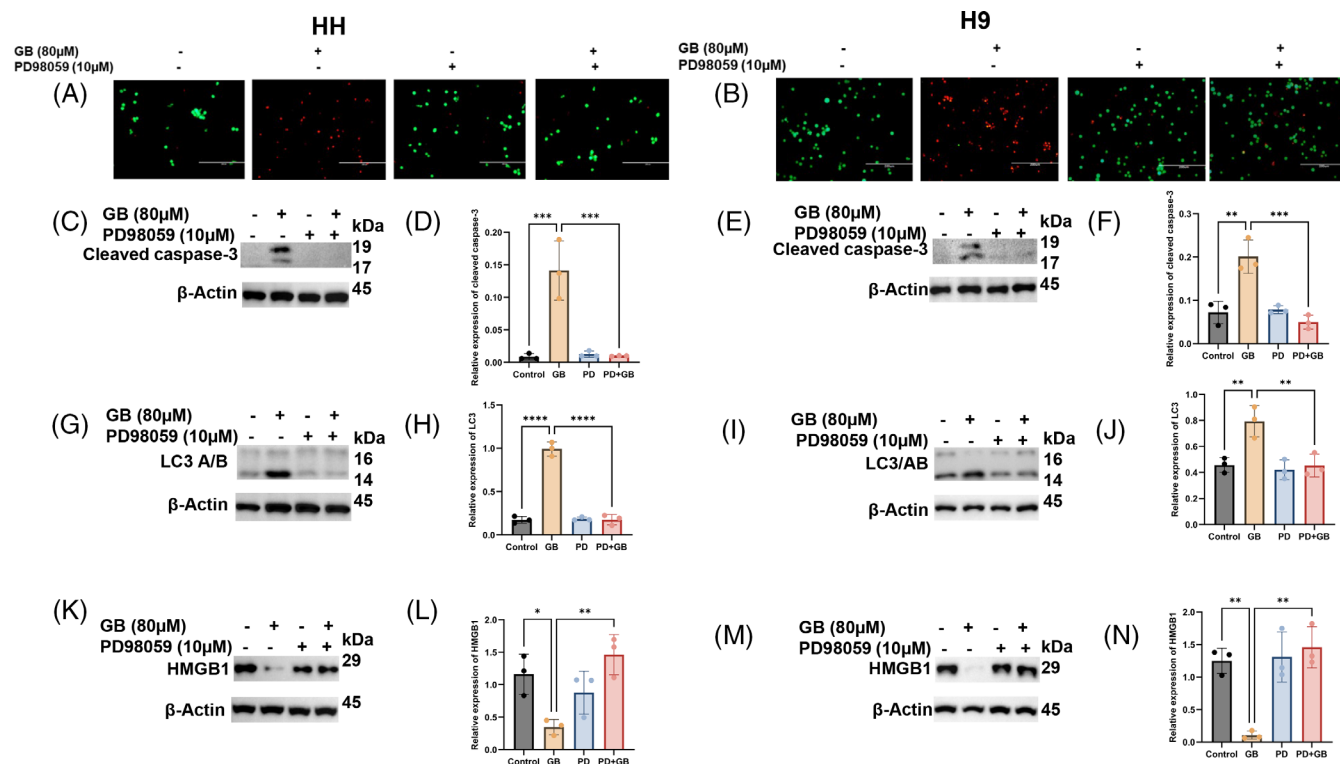


FIGURE 5 ERK inhibition prevents Glabridin induced PCD in CTCL cells. HH and H9 cells were treated with the indicated concentration of Glabridin and/or PD98059 alone and in combination. (A and B) The live and dead cell staining HH and H9 cells. For the identification of live cells, we have used green fluorescent calcein-AM dye for the intracellular esterase and red-fluorescent ethidium homodimer-1 which indicates a loss of membrane integrity (scale bar 200 μ m; magnification 20 \times). (C–N) HH and H9 cells were treated with the indicated concentration of Glabridin and/or PD98059 alone and in combination and cell lysates were prepared followed by immunoblotting. Western blot analysis of cleaved caspase 3, LC3 and HMGB1 and their relative quantification results are presented as mean \pm SD ($n = 3$). The intensity of the bands was normalized with the respective loading control and quantified using image lab software. * $p < 0.05$, ** $p < 0.01$, *** $p < 0.001$ and **** $p < 0.0001$ represent the level of significance between treatment groups relative to control (positive and negative) groups.

metabolite set enrichment analysis of the significant features in Glabridin and PD98089 + Glabridin is shown in Supplementary Figure S5B. Further, pathway analysis of Glabridin and PD98089 + GB treated cells show that thiamine metabolism, glycine, serine and threonine metabolism, glutathione metabolism, taurine and hypotaurine metabolism, and cysteine and methionine metabolism, are the five most significantly affected metabolic pathways as shown in Supplementary Figure S5C and Supplementary Table S3.

3.7 | Glabridin targets signalling pathways associated with metabolic reprogramming through ERK activation

Deregulated metabolism is a complex and heterogenic phenomenon regulated by a range of signalling mechanisms and pathways. Increasing evidence indicates that cancer cells accomplish metabolic reprogramming through various deregulated signalling mechanisms and thus ultimately acquire different hallmarks including drug resistance and poor clinical outcomes. Therefore, targeting multiple pathways and regulatory molecules associated with metabolic reprogramming is

imperative. In this line, we found that Glabridin markedly inhibited the expression of major signalling pathways such as AMPK, C-MYC, AKT and NOTCH (Supplementary Figure S7A–P) associated with metabolic reprogramming in cancer cells. Next, we further explored the role of ERK in the Glabridin-induced inhibition of these signalling pathways. Interestingly, as shown in Figure 7A–P, inhibition of ERK with PD98059 markedly reversed the expression of the above-mentioned signalling proteins in Glabridin treated CTCL cells. Hence, these findings indicate the ERK dependent multi-targeting potential of Glabridin in CTCL cells. Interestingly, we also found that Glabridin inhibits spheroid formation in CTCL cells in an ERK dependent fashion (Supplementary Figure S4B,C).

3.8 | Glabridin sensitized CTCL cells to bortezomib

Chemoresistance or resistance to anti-cancer drugs is a major challenge of cancer therapy and hence requires the exploration of novel and effective measures. Intriguingly, we investigated the sensitizing potential of Glabridin towards bortezomib in CTCL cells. As shown in Figure 8A, the CCK-8 assay reveals a significant decrease in cell

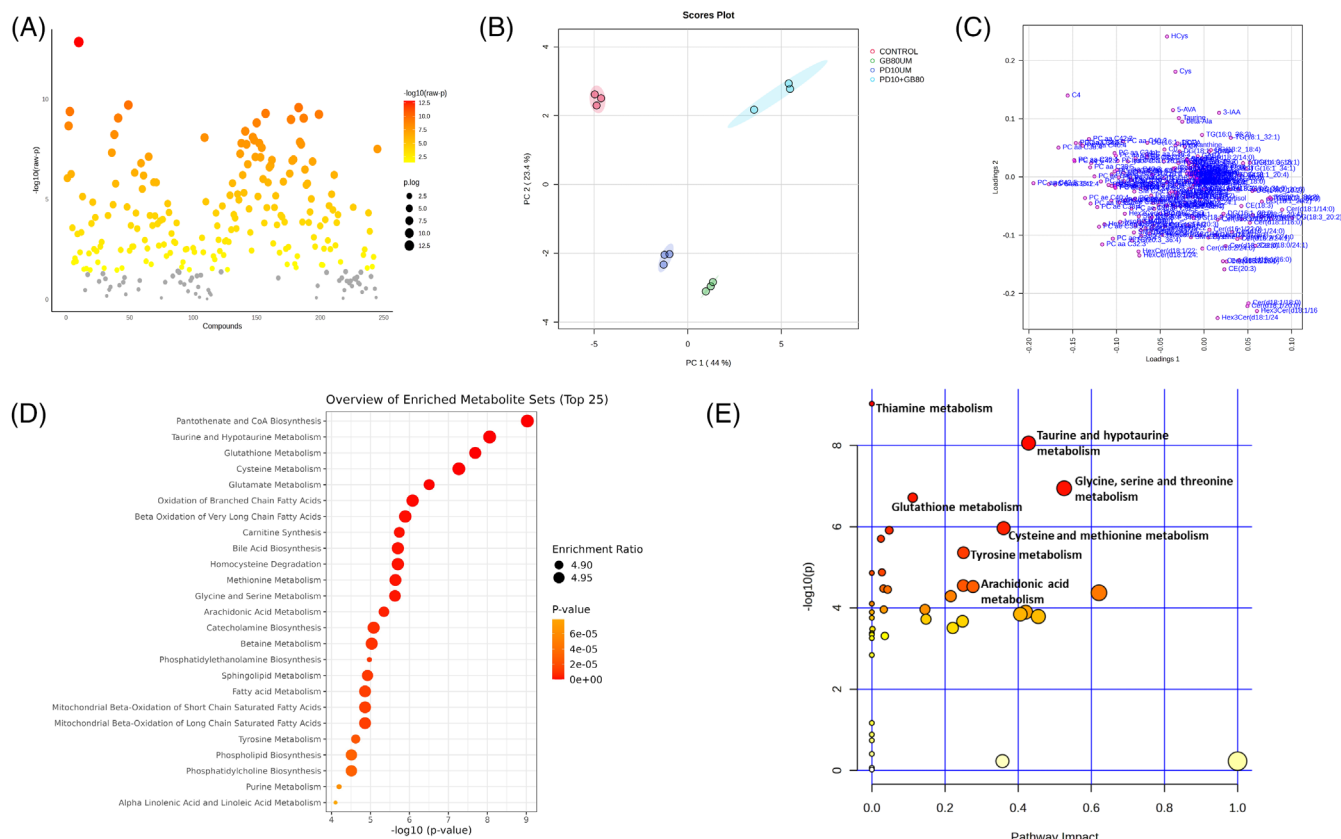


FIGURE 6 Metabolomic profiling of CTCL cells (H9) treated with Glabridin and ERK inhibitor PD98059. (A) Scatter plot showing the important features identified by ANOVA plot with $-\log_{10}p$ values on the y-axis and metabolites (compounds) on the x-axis. Coloured dots show the significant metabolites with a p -value < 0.05 . (B) Principal component analysis (PCA) of targeted metabolomics data from the samples of different experimental groups (control, Glabridin 80 μ M, PD10 μ M and PD10 μ M + Glabridin 80 μ M) of CTCL cells. (C) Loading plot of the first two principal components. Functional analysis of the significant features in Glabridin treated CTCL cells using MetaboAnalyst 6.0 (<https://www.metaboanalyst.ca/>). (D) Quantitative enrichment analysis (QEA) overview presenting the top 25 metabolic pathways. Within a particular metabolic pathway, enrichment ratio is calculated as the number of observed hits/expected hits. (E) Metabolome view of the important metabolic pathways. The pathway impact values (x-axis) represent the influencing factor of a topological analysis, and the $-\log(p)$ (y-axis) represents the p -value of the pathway enrichment analysis and pathways impact values from the pathway topology analysis, respectively.

viability in Glabridin + bortezomib treated cells as compared to only Glabridin treatment. Further, flow cytometry data depicted that Glabridin treatment sensitizes CTCL cells to bortezomib as there is a significant increase in the percentage of apoptotic cells in Glabridin + bortezomib treated cells as compared to their alone counterpart (Figure 8B,C). Furthermore, our results also showed increased expression of apoptotic and autophagy markers in CTCL cells treated with Glabridin in combination with bortezomib as compared to alone treatments (Figure 8D-K). Hence, based on these results, it can be postulated that Glabridin has strong sensitizing potential to anti-cancer drugs and thus has the potential of a suitable sensitizing agent.

4 | DISCUSSION

CTCL is an increasing health-related concern and hence, understanding the underlying mechanism associated with CTCL pathogenesis is

imperative to improve the patient's health. There is growing concern about re-investigating the role of MAPK signalling in regulating cell survival and the stemness of cancer cells. Hence in the current study for the first time, we have explored the crucial roles of MAPK pathways in regulation of the underlying mechanisms and metabolic pathways related to the orchestration of cancer hallmarks in CTCL cells treated with Glabridin.

Furthermore, there is growing concern about developing novel and effective treatment regimens with no or very minimal adverse effects. In this line, much attention has been given to natural products due to their multi-targeting nature and thus can attenuate the expression of major signalling pathways associated with cancer cell growth and stemness features. Glabridin, an active constituent of licorice (*G. glabra*) possesses a range of pharmacological actions, act through modulating various signalling pathways associated with cell proliferation, metabolism and programmed cell death.^{24,29} Indeed, the data of the current investigation demonstrated that Glabridin inhibits the

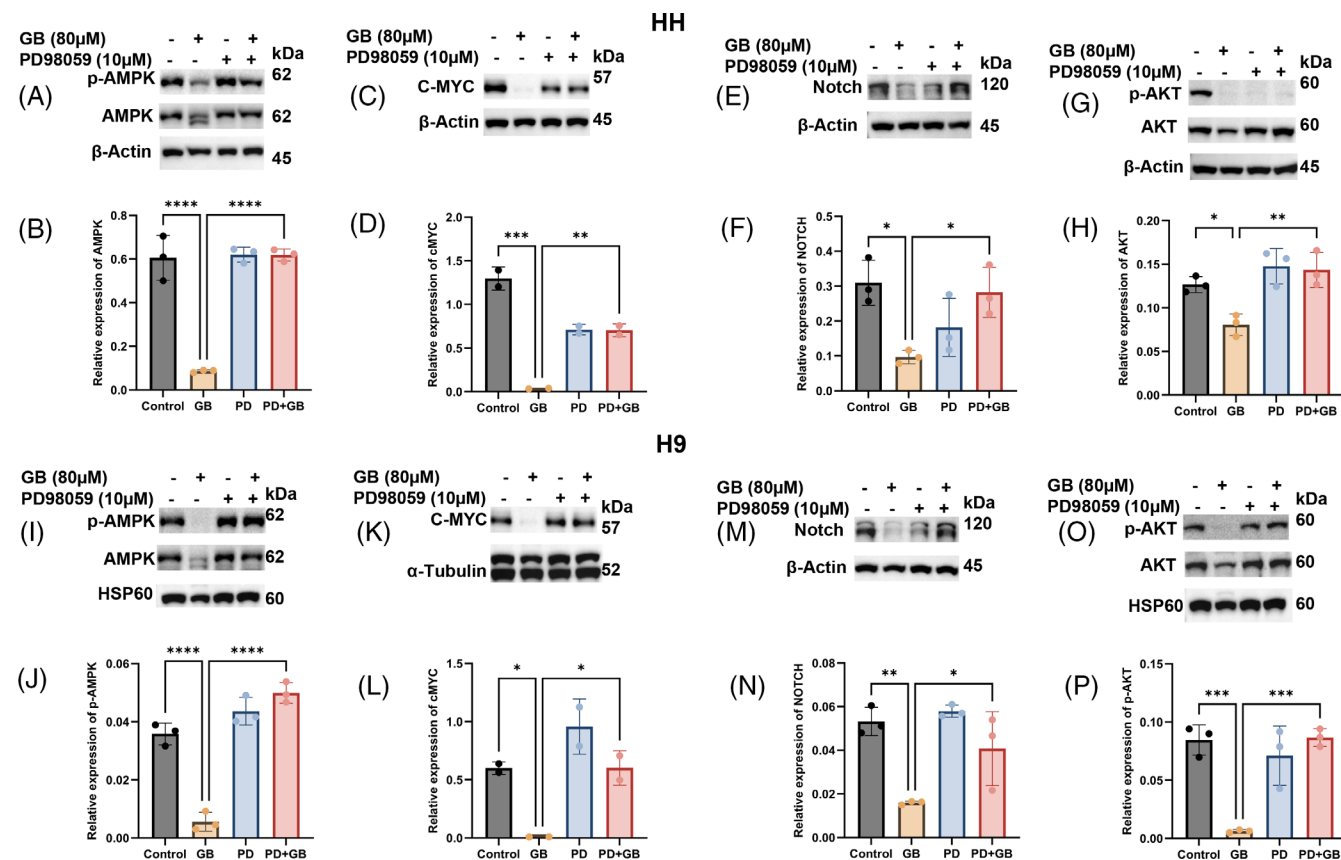


FIGURE 7 Glabridin targets signalling pathways associated with metabolic reprogramming through ERK. HH and H9 cells were treated with the indicated concentrations of Glabridin and PD98059 alone and in combination followed by cell lysates preparation and immunoblotting. (A–P) The western blot analysis of p-AMPK, AMPK, c-MYC, Notch, p-AKT and AKT and their relative quantification results are presented as mean \pm SD ($n = 2$, $n = 3$). The intensity of the bands was normalized with the respective loading control and quantified using image lab software. * $p < 0.05$, ** $p < 0.01$, *** $p < 0.001$ and **** $p < 0.0001$ represent the level of significance between treatment groups relative to control (positive and negative) groups.

growth and proliferation of human CTCL cells through PCD, which includes apoptosis, autophagy and necrosis via targeting the deregulated oncogenic signalling pathways. Interestingly, Glabridin at 40, 80 and 100 μM have already shown similar pharmacological actions (anti-tumour effect) and thus supports the findings of this study.^{33–36}

MAPK signalling is one of the most important mechanisms that regulates the developmental and physiological pathways and thus maintains cellular biological homeostasis. Interestingly, the results of this study show that ERK/MAPK is the major signalling target of Glabridin which agrees with the previous reports.^{33,36} Indeed, inhibition of ERK with PD98059 supports its role in Glabridin-induced programmed cell death in CTCL cells.

Targeting the PCD, which is the most deregulated mechanism in cancer cells, is an important strategy for the selective elimination of neoplastic cells. However, deregulation of apoptosis, autophagy and necrosis also play a key role in maintaining the cancer hallmarks, including cancer stemness and disease recurrence.³⁷ Importantly, Glabridin mediated anti-cancer actions through apoptosis, autophagy and necrosis as supported by the outcomes of this study. Further, we

also highlight the crucial role of ERK in Glabridin induced PCD of human CTCL cell lines. Importantly, Glabridin treatment also attenuates the metabolic reprogramming and stemness properties of CTCL cells through MAPK signalling pathways which agrees with earlier reports.^{38,39}

Metabolic/energy reprogramming in cancer cells is the major driving force for the uncontrolled growth, proliferation and progression of cancer cells through escaping/defeating various regulatory mechanisms including immune escape from the neighbouring non-cancerous cells like stromal immune cells.⁴⁰ Hence targeting metabolic pathways linked with cancer cells as well as normal neighbouring cells would be an important strategy for the effective elimination of cancer cells and the associated tumour microenvironment.⁴⁰ Interestingly, our metabolic profiling data indicates that Glabridin treatment markedly affected crucial metabolic pathways integral in CTCL pathogenesis and metabolic reprogramming. Moreover, metabolites, including amino acid, biogenic amines, amino acid related metabolites, fatty acids, carboxylic acids, ceramide, acylcarnitines and nucleobases and cofactors modulated by Glabridin in an ERK dependent manner suggesting an important association

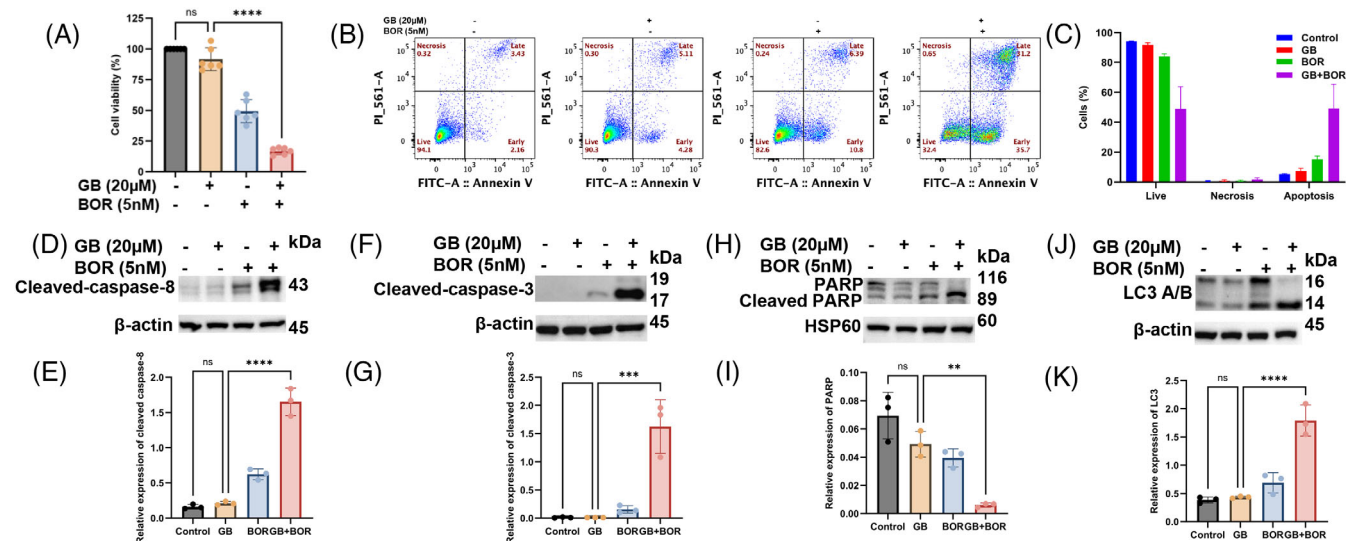


FIGURE 8 Glabridin sensitizes CTCL cells to bortezomib. (A) The effect of the indicated concentration of Glabridin and bortezomib alone and in combination on the % cell viability of H9 cells. Results are expressed as mean \pm SD ($n = 6$). (B) The representative data of H9 cells treated with the indicated concentration of Glabridin and bortezomib alone and in combination for 24 h followed by staining with fluorescein-conjugated Annexin-V/PI, and apoptotic and necrotic cells were determined by flow cytometry. (C) The percent of apoptosis and necrosis in cells of different treatment groups and the data is expressed as mean \pm SD ($n = 3$). (D–K) The western blot analysis of cleaved caspase-8, cleaved caspase-3, PARP, and LC3, and their relative quantification results are presented as mean \pm SD ($n = 3$). The intensity of the bands was normalized with the respective loading control and quantified using image lab software. ** $p < 0.01$, *** $p < 0.001$ and **** $p < 0.0001$ represent the level of significance between treatment groups relative to control (positive and negative) groups.

between cancer cell signalling and metabolic pathways. Similarly earlier report on metabolomics analysis shows that Glabridin treatment reversed the metabolic alterations induced by lipopolysaccharide (LPS) in macrophage cells.⁴¹

Amino acids (AA) and their related metabolites are the essential metabolites for the synthesis of various macromolecules including protein, lipids and nucleic acids and their upregulated level has a strong association with cancer pathobiology.⁴² Interestingly, Glabridin treatment causes increased level of fatty acids in CTCL cells which could be a potential trigger for the induction of PCD and is also supported by studies on fatty acid mediated cell death.^{43–46} Ceramides are lipids (sphingolipids) play crucial role in cell proliferation programmed cell death and metabolic reprogramming.^{47,48} Interestingly, anti-cancer agents induce PCD in cancer cells through ceramide induction which corroborates with our findings.⁴⁹ Dysregulated choline play a major role in cancer pathobiology, progression and stemness features including resistance.^{50,51} Metabolic profiling of Glabridin treated CTCL cells showed depletion in choline level in an ERK dependent manner which is supported by others.^{4,52}

In this line, adenosine 5'-monophosphate (AMP)-activated protein kinase (AMPK) is the major protein that senses and regulates cellular energy balance through monitoring energy metabolic pathways and biological functioning of mitochondria and lysosomes and thus maintains cell growth and homeostasis.^{53,54} Its role in cancer pathogenesis is not clear, as studies have shown its protumorigenic as well as anti-tumorigenic potential.^{55–57} Moreover, AMPK activation is one of the main culprits in the growth and stemness of cancer cells via metabolic reprogramming.^{58–60} Hence, targeting AMPK could be an important

measure for cancer management. Glabridin inhibits AMPK in human CTCL cells and thus supports its importance in modulating energy sensing metabolic pathways. Similarly earlier reports also revealed that AMPK inhibition suppresses cancer pathogenesis and sensitizes cancer cells to apoptosis.^{60–62} Furthermore, it has been also reported that AMPK inhibition promotes apoptosis in acute leukaemia to multiple BH3 mimetics.⁶³ Beside AMPK, recent updates also highlight the role of c-MYC, NOTCH and AKT signalling in the metabolic reprogramming of neoplastic cells.^{20,64–67} In line, Glabridin regulates these signalling pathways associated with metabolic rewiring in cancer cells through ERK activation thus supporting additional mechanisms contributing to metabolic reprogramming in cancer cells which corroborate with earlier findings.²⁶

There has been growing concern about the limitations of the current treatment options for CTCL. Adverse side effects, poor prognosis and disease recurrence are the major challenges of the clinics. In this line, a combinational therapeutic approach has given importance for better disease management. Indeed, our results further strengthened that Glabridin also sensitized the CTCL cells to bortezomib, a drug used for multiple myeloma. Importantly, Glabridin has shown no significant cytotoxic effects on normal human cells and thus indicates its potential anti-cancer importance.³³

In conclusion, mechanistic investigation as well as metabolomics profiling of Glabridin treated human CTCL cells showed a crucial role of ERK dependent pathways in regulating growth and proliferation. Thus, Glabridin through its multi-targeting nature has shown promising outcomes that can be translated for the management of CTCL patients.

AUTHOR CONTRIBUTIONS

Khan AQ: Study design, supervision, conceptualization, methodology, data collection and analysis, writing original draft, review and editing. **Agha MV, Anvar R, Khalid SA:** Data collection. **Fareed A, Mateo J:** Flow cytometry experiments and analysis. **Alam M, Buddenkotte J, Uddin S:** Visualization, writing—review and editing. **Steinhoff M:** Supervision, conceptualization, study design, writing—review and editing and resources. All authors gave their final approval and agree to be accountable for all aspects of the work.

ACKNOWLEDGEMENTS

This work was supported by the Medical Research Center (MRC-01-23-067), to Abdul Q. Khan, at Hamad Medical Corporation, Doha, Qatar. The authors thank the Qatar National Library to fund this article's open access publication charge.

CONFLICT OF INTEREST STATEMENT

The authors declare no conflicts of interest.

DATA AVAILABILITY STATEMENT

The data that support the findings of this study are available from the corresponding author upon reasonable request.

ORCID

Abdul Q. Khan  <https://orcid.org/0000-0002-5774-6845>

Shahab Uddin  <https://orcid.org/0000-0003-1886-6710>

Martin Steinhoff  <https://orcid.org/0000-0002-7090-2187>

REFERENCES

- Liu X, Jin S, Hu S, et al. Single-cell transcriptomics links malignant T cells to the tumor immune landscape in cutaneous T cell lymphoma. *Nat Commun*. 2022;13(1):1158. doi:10.1038/s41467-022-28799-3
- Hanahan D, Weinberg RA. Hallmarks of cancer: the next generation. *Cell*. 2011;144(5):646-674. doi:10.1016/j.cell.2011.02.013
- Wang W, Zou W. Amino acids and their transporters in T cell immunity and cancer therapy. *Mol Cell*. 2020;80(3):384-395. doi:10.1016/j.molcel.2020.09.006
- Xiong J, Bian J, Wang L, et al. Dysregulated choline metabolism in T-cell lymphoma: role of choline kinase- α and therapeutic targeting. *Blood Cancer J*. 2015;5(3):287. doi:10.1038/bcj.2015.10
- Yakymiv Y, Marchisio S, Ortolan E, et al. CD39/CD73 dysregulation and adenosine metabolism contribute to T-cell immunosuppression in patients with Sézary syndrome. *Blood*. 2023;141(1):111-116. doi:10.1182/blood.2022017259
- Mondal D, Shinde S, Paul S, et al. Diagnostic significance of dysregulated miRNAs in T-cell malignancies and their metabolic roles. *Front Oncol*. 2023;13:1230273. doi:10.3389/fonc.2023.1230273
- Yoshida-Sakai N, Watanabe T, Yamamoto Y, et al. Adult T-cell leukemia-lymphoma acquires resistance to DNA demethylating agents through dysregulation of enzymes involved in pyrimidine metabolism. *Int J Cancer*. 2022;150(7):1184-1197. doi:10.1002/ijc.33901
- Khan MA, Zubair H, Anand S, Srivastava SK, Singh S, Singh AP. Dysregulation of metabolic enzymes in tumor and stromal cells: role in oncogenesis and therapeutic opportunities. *Cancer Lett*. 2020;473:176-185. doi:10.1016/j.canlet.2020.01.003
- Osman AA, Arslan E, Bartels M, et al. Dysregulation and epigenetic reprogramming of NRF2 signaling axis promote acquisition of cisplatin resistance and metastasis in head and neck squamous cell carcinoma. *Clin Cancer Res*. 2023;29(7):1344-1359. doi:10.1158/1078-0432.CCR-22-2747
- Asl ER, Amini M, Najafi S, et al. Interplay between MAPK/ERK signaling pathway and MicroRNAs: a crucial mechanism regulating cancer cell metabolism and tumor progression. *Life Sci*. 2021;278:119499. doi:10.1016/j.lfs.2021.119499
- Smith LK, Rao AD, McArthur GA. Targeting metabolic reprogramming as a potential therapeutic strategy in melanoma. *Pharmacol Res*. 2016;107:42-47. doi:10.1016/j.phrs.2016.02.009
- Hargadon KM. Genetic dysregulation of immunologic and oncogenic signaling pathways associated with tumor-intrinsic immune resistance: a molecular basis for combination targeted therapy-immunotherapy for cancer. *Cell Mol Life Sci*. 2023;80(2):40. doi:10.1007/s00018-023-04689-9
- Mishra SK, Millman SE, Zhang L. Metabolism in acute myeloid leukemia: mechanistic insights and therapeutic targets. *Blood*. 2023;141(10):1119-1135. doi:10.1182/blood.2022018092
- Pavlova NN, Zhu J, Thompson CB. The hallmarks of cancer metabolism: still emerging. *Cell Metab*. 2022;34(3):355-377. doi:10.1016/j.cmet.2022.01.007
- Intlekofer AM, Finley LWS. Metabolic signatures of cancer cells and stem cells. *Nat Metab*. 2019;1(2):177-188. doi:10.1038/s42255-019-0032-0
- Malayil R, Chhichholiya Y, Vasudeva K, et al. Oncogenic metabolic reprogramming in breast cancer: focus on signaling pathways and mitochondrial genes. *Med Oncol*. 2023;40(6):174. doi:10.1007/s12032-023-02037-2
- Xiang H, Yang R, Tu J, et al. Metabolic reprogramming of immune cells in pancreatic cancer progression. *Biomed Pharmacother*. 2023;157:113992. doi:10.1016/j.biopha.2022.113992
- Arner EN, Rathmell JC. Metabolic programming and immune suppression in the tumor microenvironment. *Cancer Cell*. 2023;41(3):421-433. doi:10.1016/j.ccell.2023.01.009
- Li Y-J, Zhang C, Martincuks A, Herrmann A, Yu H. STAT proteins in cancer: orchestration of metabolism. *Nat Rev Cancer*. 2023;23(3):115-134. doi:10.1038/s41568-022-00537-3
- Hoxhaj G, Manning BD. The PI3K-AKT network at the interface of oncogenic signalling and cancer metabolism. *Nat Rev Cancer*. 2020;20(2):74-88. doi:10.1038/s41568-019-0216-7
- El-Sahli S, Wang L. Cancer stem cell-associated pathways in the metabolic reprogramming of breast cancer. *Int J Mol Sci*. 2020;21(23):9125. doi:10.3390/ijms21239125
- Papa S, Choy PM, Bubici C. The ERK and JNK pathways in the regulation of metabolic reprogramming. *Oncogene*. 2019;38(13):2223-2240. doi:10.1038/s41388-018-0582-8
- Nwosu ZC, Piorońska W, Battello N, et al. Severe metabolic alterations in liver cancer lead to ERK pathway activation and drug resistance. *EBioMedicine*. 2020;54:102699. doi:10.1016/j.ebiom.2020.102699
- Zhang J, Wu X, Zhong B, et al. Review on the diverse biological effects of Glabridin. *Drug Des Devel Ther*. 2023;17:15-37. doi:10.2147/DDDT.S385981
- Lin H, Ai D, Liu Q, et al. Natural isoflavone Glabridin targets PI3K γ as an adjuvant to increase the sensitivity of MDA-MB-231 to tamoxifen and DU145 to paclitaxel. *J Steroid Biochem Mol Biol*. 2024;236:106426. doi:10.1016/j.jsbmb.2023.106426
- Simmler C, Pauli GF, Chen S-N. Phytochemistry and biological properties of Glabridin. *Fitoterapia*. 2013;90:160-184. doi:10.1016/j.fitote.2013.07.003
- Chang J, Wang L, Zhang M, Lai Z. Glabridin attenuates atopic dermatitis progression through downregulating the TLR4/MyD88/NF- κ B

- signaling pathway. *Genes Genomics*. 2021;43(8):847-855. doi:10.1007/s13258-021-01081-4
28. Peng G, Li Y, Zeng Y, Sun B, Zhang L, Liu Q. Effect of Glabridin combined with bakuchiol on UVB-induced skin damage and its underlying mechanism: an experimental study. *J Cosmet Dermatol*. 2024;23:2256-2269. doi:10.1111/jocd.16259
 29. Li D, Fan J, Du L, Ren G. Prenylated flavonoid fractions from *Glycyrrhiza glabra* alleviate insulin resistance in HepG2 cells by regulating the ERK/IRS-1 and PI3K/Akt signaling pathways. *Arch Pharm Res*. 2024;47(2):127-145. doi:10.1007/s12272-024-01485-2
 30. Al-Tamimi M, Khan AQ, Anver R, et al. Pristimerin mediated anticancer effects and sensitization of human skin cancer cells through modulation of MAPK signaling pathways. *Biomed Pharmacother*. 2022;156:113950. doi:10.1016/j.biopha.2022.113950
 31. Hishinuma E, Shimada M, Matsukawa N, et al. Wide-targeted metabolome analysis identifies potential biomarkers for prognosis prediction of epithelial ovarian cancer. *Toxins (Basel)*. 2021;13(7):461. doi:10.3390/toxins13070461
 32. Pang Z, Lu Y, Zhou G, et al. MetaboAnalyst 6.0: towards a unified platform for metabolomics data processing, analysis and interpretation. *Nucleic Acids Res*. 2024:gkae253. doi:10.1093/nar/gkae253
 33. Huang H-L, Hsieh M-J, Chien M-H, Chen H-Y, Yang S-F, Hsiao P-C. Glabridin mediate caspases activation and induces apoptosis through JNK1/2 and p38 MAPK pathway in human promyelocytic leukemia cells. *PLoS One*. 2014;9(6):e98943. doi:10.1371/journal.pone.0098943
 34. Zhu K, Li K, Wang H, Kang L, Dang C, Zhang Y. Discovery of Glabridin as potent inhibitor of epidermal growth factor receptor in SK-BR-3 cell. *Pharmacology*. 2019;104(3-4):113-125. doi:10.1159/000496798
 35. Cui X, Cui M. Glabridin induces paraptosis-like cell death via ER stress in breast cancer cells. *Heliyon*. 2022;8(9):e10607. doi:10.1016/j.heliyon.2022.e10607
 36. Chen C-T, Chen Y-T, Hsieh Y-H, et al. Glabridin induces apoptosis and cell cycle arrest in oral cancer cells through the JNK1/2 signaling pathway. *Environ Toxicol*. 2018;33(6):679-685. doi:10.1002/tox.22555
 37. Su Z, Yang Z, Xu Y, Chen Y, Yu Q. Apoptosis, autophagy, necroptosis, and cancer metastasis. *Mol Cancer*. 2015;14:48. doi:10.1186/s12943-015-0321-5
 38. Jiang F, Li Y, Mu J, et al. Glabridin inhibits cancer stem cell-like properties of human breast cancer cells: an epigenetic regulation of miR-148a/SMA2 signaling. *Mol Carcinog*. 2016;55(5):929-940. doi:10.1002/mc.22333
 39. Wang Z, Luo S, Wan Z, et al. Glabridin arrests cell cycle and inhibits proliferation of hepatocellular carcinoma by suppressing braf/MEK signaling pathway. *Tumour Biol*. 2016;37(5):5837-5846. doi:10.1007/s13277-015-4177-5
 40. Stine ZE, Schug ZT, Salvino JM, Dang CV. Targeting cancer metabolism in the era of precision oncology. *Nat Rev Drug Discov*. 2022;21(2):141-162. doi:10.1038/s41573-021-00339-6
 41. Liu K, Pi F, Zhang H, et al. Metabolomics analysis to evaluate the anti-inflammatory effects of polyphenols: Glabridin reversed metabolism change caused by LPS in RAW 264.7 cells. *J Agric Food Chem*. 2017;65(29):6070-6079. doi:10.1021/acs.jafc.7b01692
 42. Lieu EL, Nguyen T, Rhyne S, Kim J. Amino acids in cancer. *Exp Mol Med*. 2020;52(1):15-30. doi:10.1038/s12276-020-0375-3
 43. Pompeia C, Lima T, Curi R. Arachidonic acid cytotoxicity: can arachidonic acid be a physiological mediator of cell death? *Cell Biochem Funct*. 2003;21(2):97-104. doi:10.1002/cbf.1012
 44. Lappano R, Sebastiani A, Cirillo F, et al. The lauric acid-activated signaling prompts apoptosis in cancer cells. *Cell Death Discov*. 2017;3:17063. doi:10.1038/cddiscovery.2017.63
 45. D'Eliseo D, Velotti F. Omega-3 fatty acids and cancer cell cytotoxicity: implications for multi-targeted cancer therapy. *J Clin Med*. 2016;5(2):15. doi:10.3390/jcm5020015
 46. Wang J, Chen Y, Song Q, Griffiths A, Song Z. mTORC1-IRE1 α pathway activation contributes to palmitate-elicited triglyceride secretion and cell death in hepatocytes. *Exp Biol Med (Maywood)*. 2020;245(14):1268-1279. doi:10.1177/1535370220928276
 47. Henry B, Möller C, Dimanche-Boitrel M-T, Gulbins E, Becker KA. Targeting the ceramide system in cancer. *Cancer Lett*. 2013;332(2):286-294. doi:10.1016/j.canlet.2011.07.010
 48. Morad SAF, Cabot MC. Ceramide-orchestrated signalling in cancer cells. *Nat Rev Cancer*. 2013;13(1):51-65. doi:10.1038/nrc3398
 49. Wajapeyee N, Beamon TC, Gupta R. Roles and therapeutic targeting of ceramide metabolism in cancer. *Mol Metab*. 2024;83:101936. doi:10.1016/j.molmet.2024.101936
 50. Glunde K, Penet M-F, Jiang L, Jacobs MA, Bhujwalla ZM. Choline metabolism-based molecular diagnosis of cancer: an update. *Expert Rev Mol Diagn*. 2015;15(6):735-747. doi:10.1586/14737159.2015.1039515
 51. Glunde K, Bhujwalla ZM, Ronen SM. Choline metabolism in malignant transformation. *Nat Rev Cancer*. 2011;11(12):835-848. doi:10.1038/nrc3162
 52. Pucci S, Fasoli F, Moretti M, et al. Choline and nicotine increase glioblastoma cell proliferation by binding and activating $\alpha 7$ - and $\alpha 9$ -containing nicotinic receptors. *Pharmacol Res*. 2021;163:105336. doi:10.1016/j.phrs.2020.105336
 53. Hsu C-C, Peng D, Cai Z, Lin H-K. AMPK signaling and its targeting in cancer progression and treatment. *Semin Cancer Biol*. 2022;85:52-68. doi:10.1016/j.semcancer.2021.04.006
 54. Steinberg GR, Hardie DG. New insights into activation and function of the AMPK. *Nat Rev Mol Cell Biol*. 2023;24(4):255-272. doi:10.1038/s41580-022-00547-x
 55. Sadria M, Seo D, Layton AT. The mixed blessing of AMPK signaling in cancer treatments. *BMC Cancer*. 2022;22(1):105. doi:10.1186/s12885-022-09211-1
 56. Jeon S-M, Hay N. The double-edged sword of AMPK signaling in cancer and its therapeutic implications. *Arch Pharm Res*. 2015;38(3):346-357. doi:10.1007/s12272-015-0549-z
 57. Ashrafzadeh M, Mirzaei S, Hushmandi K, et al. Therapeutic potential of AMPK signaling targeting in lung cancer: advances, challenges and future prospects. *Life Sci*. 2021;278:119649. doi:10.1016/j.lfs.2021.119649
 58. Peng B, Zhang S-Y, Chan KI, Zhong Z-F, Wang Y-T. Novel anti-cancer products targeting AMPK: natural herbal medicine against breast cancer. *Molecules*. 2023;28(2):740. doi:10.3390/molecules28020740
 59. Jeon S-M, Chandel NS, Hay N. AMPK regulates NADPH homeostasis to promote tumour cell survival during energy stress. *Nature*. 2012;485(7400):661-665. doi:10.1038/nature11066
 60. Wang Z, Wang N, Liu P, Xie X. AMPK and cancer. *Exp Suppl*. 2016;107:203-226. doi:10.1007/978-3-319-43589-3_9
 61. Viollet B, Horman S, Leclerc J, et al. AMPK inhibition in health and disease. *Crit Rev Biochem Mol Biol*. 2010;45(4):276-295. doi:10.3109/10409238.2010.488215
 62. Hu M, Chen X, Ma L, et al. AMPK inhibition suppresses the malignant phenotype of pancreatic cancer cells in part by attenuating aerobic glycolysis. *J Cancer*. 2019;10(8):1870-1878. doi:10.7150/jca.28299
 63. Jia J, Ji W, Saliba AN, et al. AMPK inhibition sensitizes acute leukemia cells to BH3 mimetic-induced cell death. *Cell Death Differ*. 2024;31(4):405-416. doi:10.1038/s41418-024-01283-9
 64. Slaninova V, Krafčíková M, Perez-Gomez R, et al. Notch stimulates growth by direct regulation of genes involved in the control of glycolysis and the tricarboxylic acid cycle. *Open Biol*. 2016;6(2):150155. doi:10.1098/rsob.150155
 65. Sellers K, Allen TD, Bousamra M, et al. Metabolic reprogramming and Notch activity distinguish between non-small cell lung cancer subtypes. *Br J Cancer*. 2019;121(1):51-64. doi:10.1038/s41416-019-0464-z

66. Lee JV, Carrer A, Shah S, et al. Akt-dependent metabolic reprogramming regulates tumor cell histone acetylation. *Cell Metab.* 2014;20(2): 306-319. doi:[10.1016/j.cmet.2014.06.004](https://doi.org/10.1016/j.cmet.2014.06.004)
67. Dong Y, Tu R, Liu H, Qing G. Regulation of cancer cell metabolism: oncogenic MYC in the driver's seat. *Signal Transduct Target Ther.* 2020;5(1):124. doi:[10.1038/s41392-020-00235-2](https://doi.org/10.1038/s41392-020-00235-2)

SUPPORTING INFORMATION

Additional supporting information can be found online in the Supporting Information section at the end of this article.

How to cite this article: Khan AQ, Agha MV, Ahmad F, et al. Metabolomics analyses reveal the crucial role of ERK in regulating metabolic pathways associated with the proliferation of human cutaneous T-cell lymphoma cells treated with Glabridin. *Cell Prolif.* 2024;57(9):e13701. doi:[10.1111/cpr.13701](https://doi.org/10.1111/cpr.13701)